

# Realistic simulations of two dimensional magnetic domain patterns

E. A. Jagla

*The Abdus Salam International Centre for Theoretical Physics  
Strada Costiera 11, (34014) Trieste, Italy*

(Dated: December 2, 2024)

I show that a minimal model for the interaction of magnetic domains, that includes a short range rigidity and a long range dipolar interaction, can reproduce most of the known phenomenology of two dimensional magnetic domain patterns. In particular bubble and stripe phases are obtained, along with (metastable) polygonal and labyrinthine morphologies. In addition, two puzzling phenomena, namely the so called ‘memory effect’ and the ‘topological melting’ observed experimentally are also accurately described. Very similar phenomenology occurs in the case in which the model is changed to be represented by the Swift-Hohenberg equation driven by an external orienting field.

PACS numbers:

## I. INTRODUCTION

There is a surprisingly large number of systems that exhibit macroscopic textures arising from microscopic interactions.<sup>1</sup> To be concrete, I will take as a case of study that of patterns in magnetic systems (magnetic garnets<sup>2</sup> or ferrofluids<sup>3</sup>), but many of the conclusions obtained can be directly applied to other systems, as for instance, the mixed state of type I superconductors of slab geometry,<sup>4</sup> and Langmuir monolayers.<sup>5</sup> The phenomenology of these systems is qualitatively understood as appearing from the competition of two effects: a short range rigidity, and a long range (dipolar) interaction between the local magnetization at different spatial positions. Calculations suggest<sup>6</sup> that the ground state of the system consists of (i) a state of uniform magnetization, (ii) a hexagonal lattice of bubbles of one sign magnetization in a background with opposite magnetization, or (iii) a phase with alternating, parallel stripes of opposite magnetization. The parameter controlling which of these three is actually the ground state is the external magnetic field. However, in experiments, upon variation of the external field, different *metastable* flux configurations develop that originate in instabilities of the bubbles or the stripes. Most noticeable, these metastable configurations include labyrinthine phases of interpenetrating domains, and polygonal-like patterns.<sup>1</sup>

Model Hamiltonians that take into account the two relevant energy scales have been used to reproduce most of the elemental instabilities observed in experiments, in particular: the elongation and ‘fingering’ instability of bubbles,<sup>7</sup> and the undulation instability of stripes.<sup>8</sup> However, the much richer behavior of the full system, appearing from complex interaction effects in rather large spatial regions has not been studied in detail with this kind of models. In fact, it is not known if these simple models contain all necessary ingredients to produce realistic magnetization patterns over large spatial scales.

The main motivation of the present work is to present realistic simulations in sufficiently large systems using a minimal model Hamiltonian to see whether they can account for the full phenomenology and the variety of mor-

phologies observed. I claim that the answer is positive, and that most of the large scale phenomenology of magnetic domain patterns are very well reproduced in numerical simulations using a minimal Hamiltonian. The success of the present simulations rely in a few tricks (some of them purely numerical, and others with more physical content) that will be discussed in the next section. The simulations are extremely precise in reproducing in particular two phenomena that have been observed in these systems and have remained largely as puzzles, namely, the so called ‘memory effect’ of some magnetic patterns, and the ‘topological melting’ of an ordered lattice of bubbles.

## II. DETAILS ON THE MODEL AND THE NUMERICAL TECHNIQUE

The model I will use is not at all new (see [1] and References therein). I will consider a scalar field  $\phi(\mathbf{r})$  defined over the  $x$ - $y$  plane. This variable will represent the magnetization in the system, that in experiments is typically constrained (because of structural properties) to point perpendicularly to the  $x$ - $y$  plane. Then, experimentally, the magnetization  $\phi$  has a preference to take two different values, that without loss of generality I will assume to be  $\pm 1$ . It will be convenient for the simulations to consider  $\phi$  as a continuum variable and include in the Hamiltonian a local term  $H_l$  that favors the values  $\phi = \pm 1$ . This term will be of the form

$$H_l = \alpha_0 \int d\mathbf{r} \left( -\frac{\phi(\mathbf{r})^2}{2} + \frac{\phi(\mathbf{r})^4}{4} \right) - h_0 \int d\mathbf{r} \phi(\mathbf{r}) \quad (1)$$

and represents the simplest continuum field description of an Ising variable. Note that a term describing the effect of an external magnetic field  $h_0$  has been already included.

The other terms that will be included in the Hamiltonian are the following. First, there is a rigidity term  $H_{rig}$  of the form

$$H_{rig} = \beta \int d\mathbf{r} \frac{|\nabla \phi(\mathbf{r})|^2}{2} \quad (2)$$

This term (with positive  $\beta$ ) discourages spatial variations of  $\phi$ , and can be called ‘attractive’, in the sense that two regions with a value of  $\phi$  of plus (or minus) one, in a background of the opposite sign, tend to merge into a single one to reduce the value of this term (in fact, in a description in terms of an Ising variable on a lattice, this term maps onto a ferromagnetic interaction between nearest neighbor sites). The fact that our fundamental variable  $\phi$  is continuous rather than discrete, and the existence of the gradient term, imply in particular the existence of a natural width (of the order of  $\sqrt{\beta/\alpha_0}$ ) for the interface between domains with positive and negative magnetization. Choosing the parameters in such a way that this width is a few times the discretization distance in the simulation, allows to obtain a smooth interface between domains, which is very weakly pinned by the underlying numerical mesh, and whose energy is almost independent of its orientation. These two facts are crucial for a realistic simulation, and cannot be easily achieved using a Ising variable that takes only two values (see for instances the attempts in [9] and [10]).<sup>11</sup>

Secondly, there is a term  $H_{dip}$  that models the dipolar interactions, of the form

$$H_{dip} = \gamma \int d\mathbf{r} d\mathbf{r}' \phi(\mathbf{r}) \phi(\mathbf{r}') G(\mathbf{r}, \mathbf{r}') \quad (3)$$

where  $G(\mathbf{r}, \mathbf{r}') \sim 1/|\mathbf{r} - \mathbf{r}'|^3$  at long distances. At short distances however, the  $r^{-3}$  behavior has to be cut off to avoid divergences (in experiments, the cut off distance is given roughly by the thickness of the film). In the simulations below, I will take  $G(\mathbf{r}, \mathbf{r}') = 1/|\mathbf{r} - \mathbf{r}'|^3$  for any two points such that  $\mathbf{r} \neq \mathbf{r}'$  (the overall intensity is controlled by the factor  $\gamma$  in Eq. (3)), whereas  $G(\mathbf{r}, \mathbf{r}) \equiv 0$ . Then the cut off distance is the lattice discretization. However, we can see that the way in which the cut off is done is not crucial for the results. In fact, we will take advantage of the fact that the two terms (2) and (3) can be compactly written in Fourier space as

$$H_{rig} + H_{dip} = \sum_{\mathbf{k}} |\phi(\mathbf{k})|^2 (\beta k^2 + \gamma G_{\mathbf{k}}) \quad (4)$$

Then, it is the combination  $(\beta k^2 + \gamma G_{\mathbf{k}})$  that will mostly determine the behavior of the system. Note that the short distance behavior of  $G$  in real space is masked in Fourier space at large  $k$  by the  $k^2$  term, and then is irrelevant. On the other hand, the  $r^{-3}$  behavior at long distances transforms into a  $k$  dependence of the form  $a_0 - a_1|k|$  in Fourier space. The constants can be exactly evaluated to be

$$\begin{aligned} a_0 &= 2\pi\gamma \int_0^\infty r dr G(r) \\ a_1 &= 2\pi\gamma \end{aligned} \quad (5)$$

Note that the finite value  $a_0$  of  $G_{\mathbf{k}}$  at  $k = 0$  reflects the fact that the interaction in real space is integrable (in spite of being sometimes called ‘long range’), and that

$a_1$  is independent of the short distance behavior of  $G(r)$ . The main features of the interaction in Fourier space are a cusp at  $k = 0$ , and a minimum at a finite wave number  $k_{min} \sim \gamma/\beta$ . This minimum exists for any non-zero  $\gamma$ , indicating that the effect of the dipolar interactions can never be neglected at large distances.

Having defined the energy function of the system, we have to introduce the dynamics. Since in magnetic systems the magnetization is a non-conserved order parameter, I will use the Allen-Cahn<sup>12</sup> dynamic equations, namely

$$\begin{aligned} \frac{\partial \phi(\mathbf{r})}{\partial t} &= -\lambda \frac{\delta(H_l + H_{rig} + H_{dip})}{\delta \phi(\mathbf{r})} = \\ &= -\lambda \left( \alpha_0(-\phi + \phi^3) - h_0 - \beta \Delta \phi + \gamma \int d\mathbf{r}' \phi(\mathbf{r}') G(|\mathbf{r} - \mathbf{r}'|) \right) \end{aligned}$$

that represents an overdamped dynamics in which the system tries to reduce its energy as much as possible. To efficiently implement these equations in the computer, and in order to avoid the direct evaluation of the integral in the last term of (6), I use the previous equation but written in the Fourier space, namely

$$\frac{\partial \phi_{\mathbf{k}}}{\partial t} = -\lambda [\alpha_0(-\phi + \phi^3)|_{\mathbf{k}} - h_0 + (\beta k^2 + \gamma G_{\mathbf{k}})\phi_{\mathbf{k}}] \quad (7)$$

In this way, the last term is now algebraic. The complication has been translated to the first term, that involves the evaluation of the Fourier transform of  $\phi^3$ . However, this can be done very efficiently by the use of standard fast-Fourier-transform techniques.

Two of the numerical coefficients in (7) can be fixed by setting new spatial and temporal scales. The evolution equation can be conveniently written in dimensionless form as

$$\frac{\partial \phi_{\mathbf{k}}}{\partial t} = \alpha(\phi - \phi^3)|_{\mathbf{k}} + h - (k^2 + G_{\mathbf{k}})\phi_{\mathbf{k}} \quad (8)$$

where new (dimensionless) constants  $\alpha$  and  $h$  have been defined. This equation has, in addition to the external control parameter  $h$ , a single internal control parameter  $\alpha$ . This parameter regulates the possibility of the field  $\phi$  to take values other than the most convenient ones, namely  $\phi = \pm 1$ . We will see below the different morphologies that appear for different values of  $\alpha$ . From now on I will always refer to the dimensionless form (8) of the equations of motion.

Starting from an arbitrary initial condition, Eq. (8) describes an evolution in which the total energy of the system  $H_l + H_{rig} + H_{dip}$  is steadily reduced until it reaches a minimum, in which  $\partial \phi_{\mathbf{k}}/\partial t$  is identically zero. We will see that typically the true minimum of the system is not reached, but instead one of many possible metastable states is obtained.

In addition, I have observed that the convergence of Eq. (8) to the local minimum can be very slow. A trick

can be implemented to speed up this convergence without changing the essence of the results obtained. It consists in including a mass term for the field  $\phi$ . Concretely the equations (8) are modified to

$$\nu \frac{\partial^2 \phi_{\mathbf{k}}}{\partial t^2} + \frac{\partial \phi_{\mathbf{k}}}{\partial t} = F_{\mathbf{k}} \quad (9)$$

where  $F_{\mathbf{k}}$  is the same right hand side term as in (8). By changing  $\nu$ , we pass from the realistic, completely overdamped dynamics for  $\nu = 0$ , to a non-dissipative (inertial) dynamics for  $\nu \rightarrow \infty$  (with the time unit properly redefined). Comparison of the results with different values of  $\nu$  (one example is shown below) show that the inclusion of a non-zero value of  $\nu$ , if not too large, can efficiently speed up the simulations without altering the essence of the results. The simulations presented below were down on a  $512 \times 512$  system using periodic boundary conditions. To obtain the results in each of the figures presented (implying a full sweep of the external field) about 10 hours of CPU time on a desktop computer were needed.

### III. RESULTS

The initial condition for the variable  $\phi$  is taken to be locally random in the interval  $-1 < \phi < 1$ , and the system is evolved until a stable configuration is reached in the presence of a finite external field  $h$ . If  $h$  is too large, the final configuration turns out to be a state of uniform magnetization. However, if the simulation is done using a lower field, a structure of bubbles of the minority phase (with magnetization anti-parallel to the field) within a background of the opposite magnetization may be favored. First of all I will show an example comparing the case of zero mass dynamics ( $\nu = 0$ ) with one of finite ( $\nu \neq 0$ ) mass of the field  $\phi$ . Fig. 1 shows the evolution of the total energy of the system in the two cases, and the configurations reached, starting from the same random configuration. The energy can be proved to be a non-increasing function of the simulation time only for  $\nu = 0$ . We see however that for the value of  $\nu$  used, energy is still essentially a decreasing function, namely we are still in an overdamped regime. In addition, the time needed to attain convergence is reduced by a factor of  $\sim 50$  when the mass term is included. The two snapshots show the same qualitative structure of bubbles of the minority phase onto a background of the opposite sign. Actually the energy evolution in the zero mass case shows that fully convergence after  $6 \times 10^4$  time steps has not been achieved, and this is seen in the corresponding pattern which shows still larger disorder than the one using the mass term after only about 700 steps. In all the simulations in the rest of the paper, a value of  $\nu$  in the range 10-500 is used.

Once the bubble pattern is obtained, the field is reduced slowly to zero and then increased with the opposite

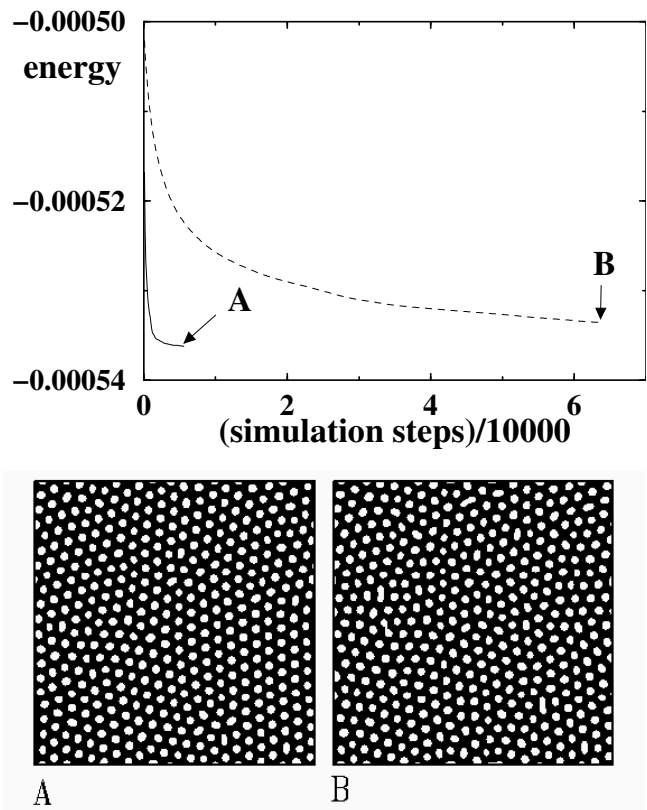


FIG. 1: Evolution of the energy per site as a function of simulation steps, starting from the same initial random conditions, for the strict overdamped dynamics ( $\nu = 0$ , dotted line), and with the inclusion of an inertia term ( $\nu = 500$ , continuous line), with  $\alpha = 1.6$  and  $h = 0.01$ . The snapshots indicate that the system converges to qualitatively the same pattern in both cases, but the convergence time has improved by a factor of  $\sim 50$  by the use of the inertia term (in all snapshots throughout the paper, black (white) represents positive (negative) magnetization).

sign, and the evolution of the system is followed. Different morphologies are observed for different values of  $\alpha$  in Eq. (8).

*Almost reversible interconversion of bubbles and stripes.* For  $\alpha = 1.6$ , the result obtained is shown in Fig. 2. Starting from the bubble phase, upon reduction of the field  $h$ , neighbor bubbles coalesce, forming a striped pattern. Due to the defects in the original structure, the stripes are oriented in different directions in different parts of the sample. When the field is inverted, the stripes destabilize, and separate in a chain of bubbles, with opposite magnetization with respect to the original ones. The sequence of bubble and stripe patterns is found to be reversible upon cycling of the field. There is however a noticeable hysteresis in the field value at which the bubble-stripe interconversion occurs. This is just the consequence of the transition between bubbles and stripes being first order.<sup>6</sup>

*From bubbles to rather isolated and wandering stripes.* For a slightly larger value of  $\alpha$ , namely  $\alpha = 1.8$  (Fig. 3),

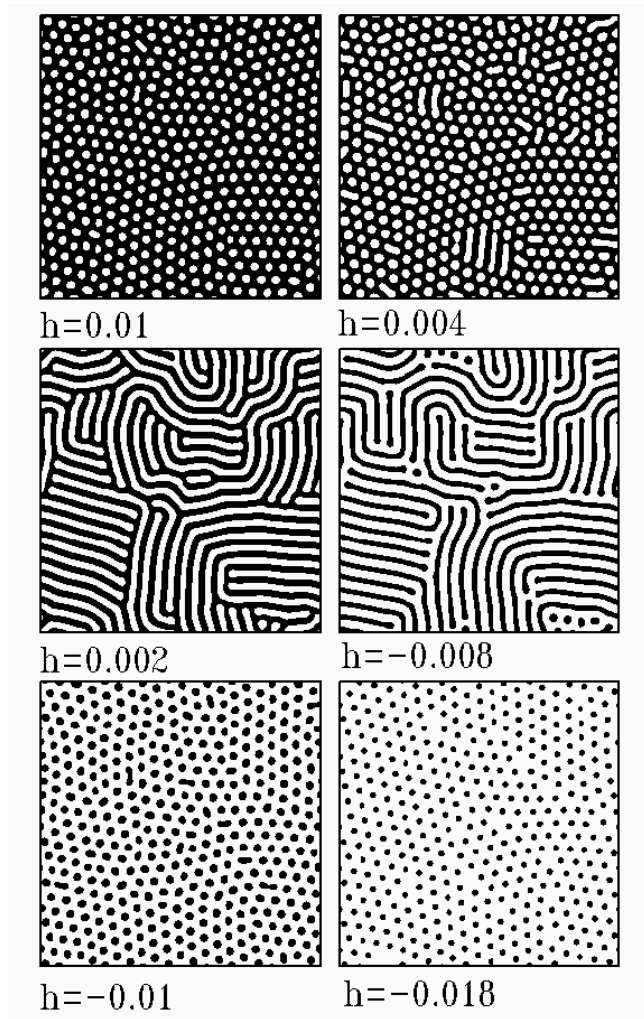


FIG. 2: Evolution of the magnetization distribution upon reduction of the magnetic field  $h$  as indicated, for  $\alpha = 1.6$ .

the bubbles may become unstable and elongate individually, without merging with their neighbors at the beginning. When they finally merge (for  $h \lesssim -0.08$ ), regions with positive magnetization generate wavy stripes of well defined thickness. Contrary to the previous case, these regions do not separate into ‘beads’ when the field is made more negative, but eventually retract back to a single spot of positive magnetization that eventually disappears.

*Collapse of the bubbles to a polygonal pattern.* For larger values of  $\alpha$ , the bubbles are seen to remain (meta) stable up to a point where they again merge with their neighbors, but now in a sort of two dimensional way, then generating a polygonal pattern as seen in Fig. 4 for  $\alpha = 2.2$ . This has to be compared with the previous case where the initial collapse of bubbles was mainly one-dimensional, generating stripes (see the case  $h = -0.02$  in Fig. 3). In the present case, the transition seems to occur as a cascade process, where some initial coalescences trigger the full transition of the lattice. In fact, if a per-

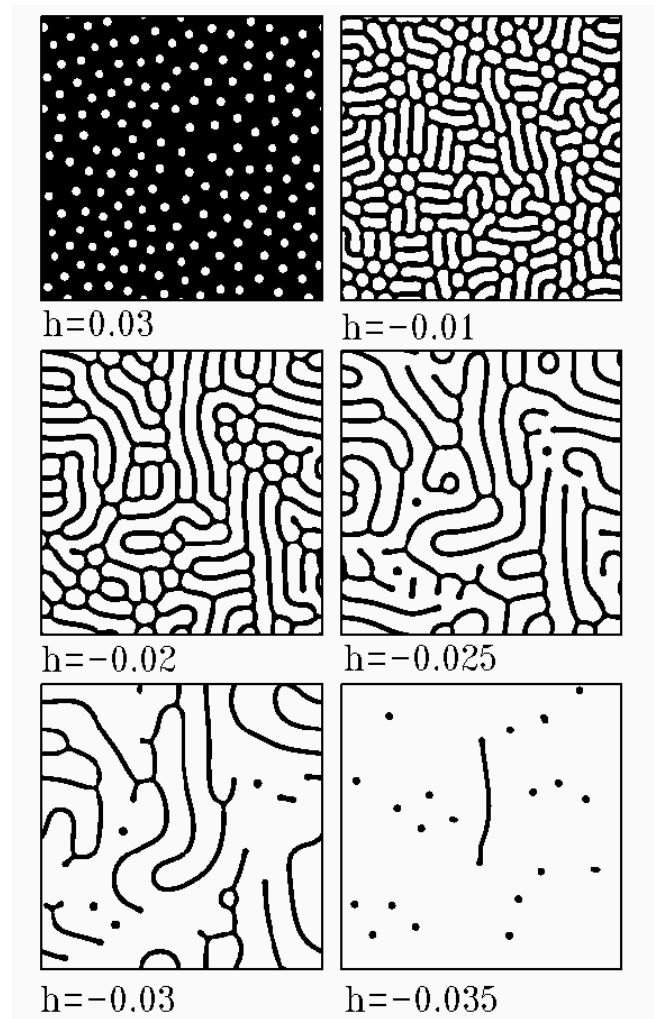


FIG. 3: Same as Fig. 2 for  $\alpha = 1.8$ .

fect original pattern of bubbles is constructed by hand, it can remain stable for values of the field at which the disordered bubble system would have already collapsed. Now, if in this perfect, metastable structure, a defect is introduced, it can completely disorder the lattice. In fact, we see in Fig. 5 how the presence of the defect produces a sequence of instabilities that destroy many of the stripes that originally separate bubbles, generating a well defined disordering front that leaves behind a disordered structure with much lower magnetization. This effect has been experimentally observed and called *topological melting*<sup>13</sup> of the bubble lattice.

Incidentally note in the last two panels of Fig. 5, the stability of the small pentagonal bubble highlighted by the arrow. These small pentagonal bubbles have been observed experimentally to be ubiquitous.<sup>13</sup>

*Memory effect and labyrinthine patterns.* If from the last pattern in Figs. 3 or 4 the field is slowly switched off, a very interesting result is observed, which is shown in Figs. 6 and 7. The stripes undergo an undulation instability,<sup>8</sup> increasing its length and meandering

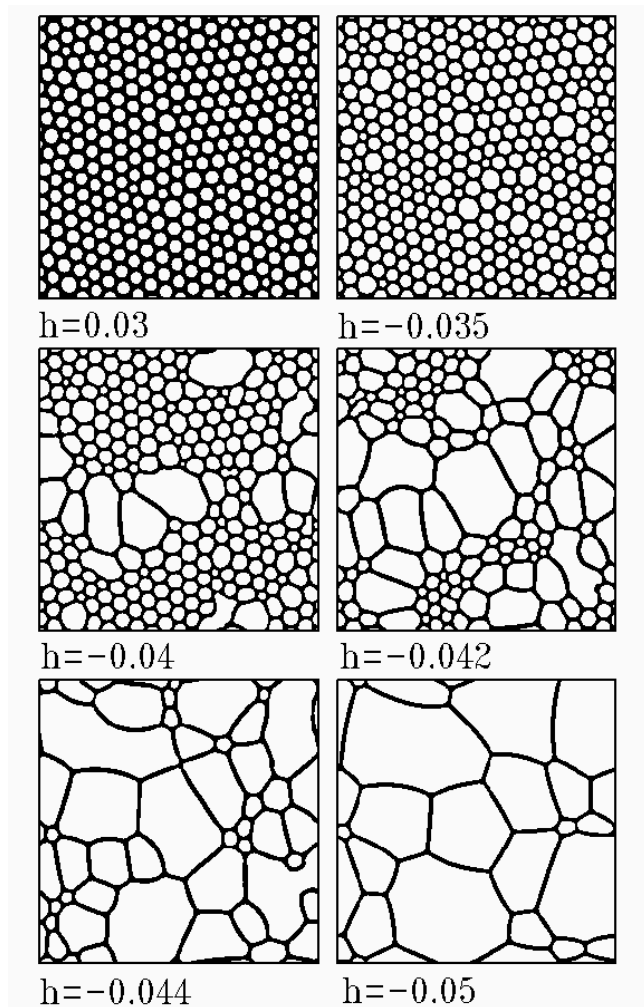


FIG. 4: Same as Fig. 2 for  $\alpha = 2.2$ .

throughout the whole system, forming a labyrinthine pattern. In particular, in the case of Fig. 7 in which the original pattern is polygonal, the undulation occur without further breaking or reconnections of any stripes, then the final labyrinthine pattern at  $h = 0$  is topologically equivalent to the original one. A nice consequence of this, is that when the field is switched on again (last panels in 7), the original pattern is almost recovered. This effect, called the *memory effect*<sup>14</sup> has been observed experimentally, and the typical evolution of the patterns over many cycles of the field has been analyzed. We are seen that this effect is contained with great detail in the very simple minimal model Hamiltonian we are using.

#### IV. DISCUSSION AND CONCLUSIONS

Summarizing, in the previous Section I have shown how the model equations (8) can be efficiently simulated in systems of reasonably large size. In this way, we have seen emerging most of the phenomenology of two dimen-

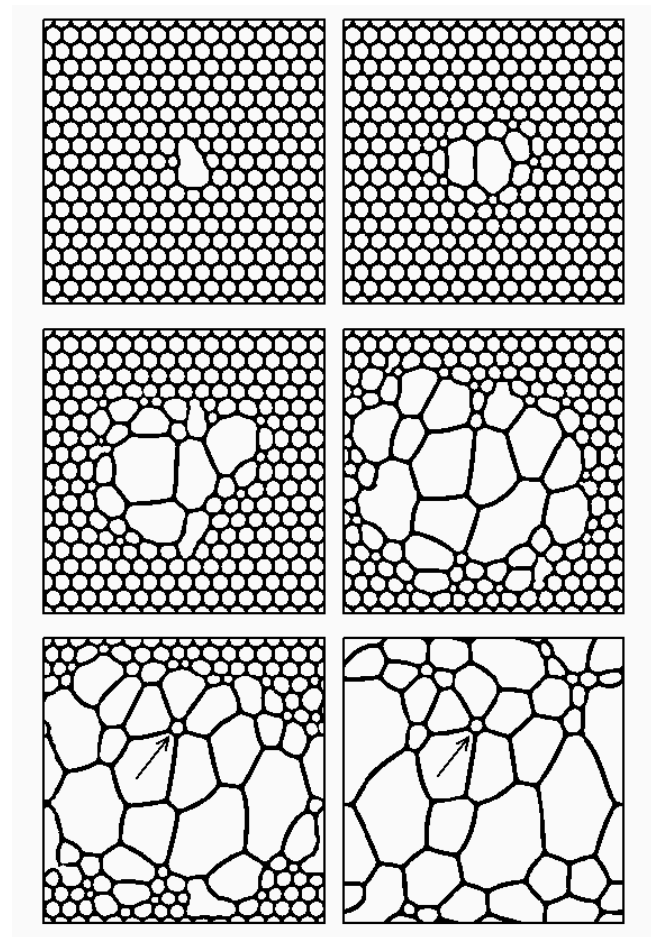


FIG. 5: Topological melting of an order array of bubbles for  $\alpha = 2.2$  and  $h = -0.045$ , upon the *ad hoc* inclusion of a defect in the middle of the sample. The evolution here occurs at a *fixed* value of the field, as a function of the simulation time. Arrows highlight a small pentagonal bubble, a structure that appears ubiquitous both in experiments and in the simulations.

sional magnetic patterns and other similar systems. The success of the present numerical simulations are due to a combination of reasons, mainly: (i) use of a continuum variable instead of a discrete one. This allows to obtain smooth domain walls between regions with opposite values of  $\phi$ , and these domain walls can move easily to minimize the energy of the system; (ii) fast-Fourier-transform techniques allow the efficient evaluation of the ‘long-range’ dipolar force; and (iii) the mass term added to the field speeds up the simulations by a large factor without spoiling the results. All these facts combine to allow a realistic simulation of domain patterns that show many of the features observed in experimental realizations. In particular, the *memory effect*<sup>14</sup> and the *topological melting*<sup>13</sup> of the system are very well reproduced.

I want to emphasize that in all cases, the evaluation of the total energy of the system shows that the only patterns truly corresponding to the ground state of the system are: (i) a pattern with uniform magnetization if

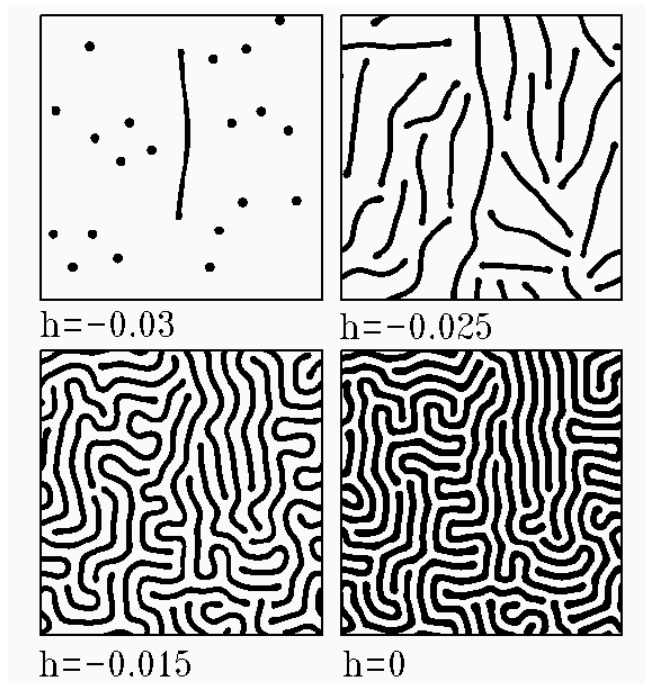


FIG. 6: Reducing the field from the final configuration in Fig. 3 down to  $h = 0$ .

the field is strong enough, (ii) a regular bubble phase for intermediate fields, and (iii) a regular stripe phase for low (including zero) field. This agrees with the results of theoretical studies.<sup>6</sup> All other patterns observed (labyrinthine, polygonal, etc.) are only metastable, and they are originated in the particular cycling of the field (and in the initial conditions) to which the sample is subjected. A recent experimental study<sup>15</sup> has shown in fact how the labyrinthine patterns converge to parallel stripes upon relaxation.

Very different morphologies have been observed when the parameter  $\alpha$  in Eq. 8 is changed. Figs. 4, 5, and 7 (corresponding to the largest values of  $\alpha$ ) compare very well with the patterns observed in magnetic garnets and ferrofluids (see [1], [13], and [14]). The results for lower  $\alpha$  (in particular, the last few panels in Fig. 3) contain more wandering stripes, and are more akin to Langmuir monolayers<sup>5</sup> and flux structures in type I superconductors.<sup>4</sup> This suggests that in real systems the possibility of the order parameter to take values different than the two preferred ones can influence noticeable the physical properties.

We have seen that in our model the dynamics is controlled by an interaction function in  $k$  space that has a cusp at  $k = 0$  and a minimum at a finite  $k_{min}$  value. It is worth comparing this case with other well known cases. One is the case in which the field  $\phi$  is considered to be charged, instead of having a magnetization. Two cases can be considered. One is that of truly three dimensional charges ( $G(r) \sim r^{-1}$ ) and the other is the case of two dimensional charges ( $G(r) \sim -\ln(r)$ ). This last case can

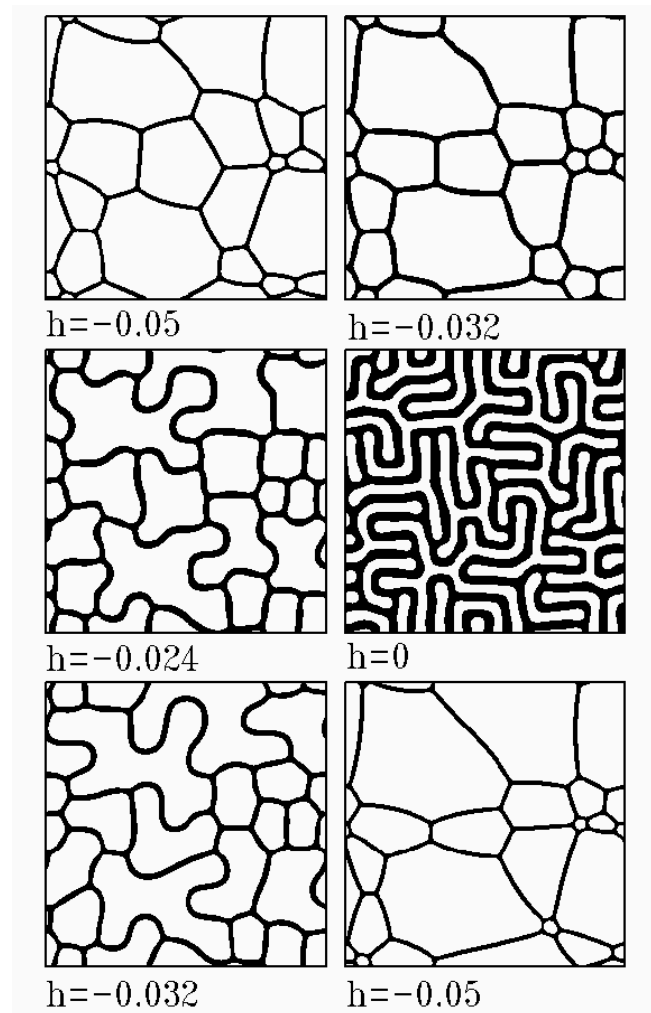


FIG. 7: Reducing the field from the final configuration in Fig. 4 down to  $h = 0$  and back to its original value. Note the ‘memory’ of the pattern as comparing first and last panels.

be seen to describe for instance the elastic interaction with a substrate, in the case in which the variable  $\phi$  represents the local density of the system.<sup>16</sup> In both cases, the interaction in  $k$  space gets a divergence at low  $k$ . The case of three dimensional charges has been studied in [17] There, instabilities of a single bubble have been found which are similar to those in dipolar systems.

Another case to compare with is that of interactions decaying in real space more rapidly than  $r^{-3}$ . In this case, a  $k$  space interaction with a quadratic maximum at  $k = 0$  is obtained. If this maximum dominates over the quadratic minimum coming from the  $\Delta\phi$  term in (6), then the effective interaction has a quadratic maximum at the origin and a minimum at some finite  $k_{mim}$ . This case corresponds qualitatively to the interaction considered in the Swift-Hohenberg equation.<sup>18</sup> For this interaction, and controlling the same parameter  $\alpha$  as I did here, I have obtained again basically all the effects and morphologies described in the previous section. On one

hand this tells that the cusp at  $k = 0$  of the dipolar interaction is not crucial in obtaining these effects, a quadratic maximum suffices. On the other hand it is a bit surprising that in the wide literature related to the Swift-Hohenberg equation these effects have not been described previously. This might be due to the fact that the Swift-Hohenberg equation is usually considered in the absence of a ‘magnetic-field-like’ term that favors one of the

two orientations, and this term is crucial to obtain the metastable patterns. It is then likely that the much studied relaxation to equilibrium properties of the patterns seen in the Swift-Hohenberg equation and the coarsening properties of the magnetic patterns (studied for instance in [14]) can be put under the same framework. I hope the present work encourages some studies in this direction.

- 
- <sup>1</sup> M. Seul and D. Andelman, *Science* **267**, 476 (1995); F. Elias, C. Flament, J.-C. Bacri, and S. Neveu, *J. Phys. I France* **7**, 711 (1997).
- <sup>2</sup> M. Seul, L. R. Monar, L. O’Gorman, and R. Wolfe, *Science* **254**, 1616 (1991); M. Seul and W. Wolfe, *Phys. Rev. A* **46**, 7519 (1992); *ibid.* **46**, 7534 (1992).
- <sup>3</sup> R. E. Rosensweig, *Sci. Am.* **247**, 124 (October 1982).
- <sup>4</sup> R. Huebener, *Magnetic Structures in Superconductors*, Springer-Verlag, Berlin (1979); A. Dorsey and R. E. Goldstein, *Phys. Rev. B* **57**, 3058 (1998); H. Bokil and O. Narayan, *Phys. Rev. B* **56**, 11195 (1997).
- <sup>5</sup> D. J. Keller, H. M. McConel, and V. T. Moy, *J. Phys. Chem.* **90**, 2311 (1986); D. Andelman, F. Brochard and J.-F. Joanny, *J. Chem. Phys.* **86** 3673 (1987); M. Seul and M. J. Sammon, *Phys. Rev. Lett.* **64**, 1903 (1990); K. J. Stine, S. A. Rauseo, B. G. Moore, J. A. Wise, and C. M. Knobler, *Phys. Rev. A* **41**, 6884 (1990); M. Seul and V. S. Chen, *Phys. Rev. Lett.* **70**, 1658 (1993).
- <sup>6</sup> T. Garel and S. Doniach, *Phys. Rev. B* **26**, 325 (1982); K.-O. Ng and D. Vanderbilt, *Phys. Rev. B* **52**, 2177 (1995); R. de Koker, W. Jiang, and H. M. McConnell, *J. Phys. Chem.* **99**, 6251 (1995).
- <sup>7</sup> S. A. Langer, R. Goldstein, and D. P. Jackson, *Phys. Rev. A* **46**, 4894 (1992); D. P. Jackson, and R. E. Goldstein, and A. O. Cebers, *Phys. Rev. E* **50**, 298 (1994); J. A. Miranda, and M. Widom, *Phys. Rev. E* **55**, 3758 (1997); D. P. Jackson and B. Gantner, *Phys. Rev. E* **64**, 056230 (2001).
- <sup>8</sup> F. Elias, I. Drikis, A. Cebers, C. Flament, and J.-C. Bacri, *Eur. Phys. J. B* **3**, 203 (1998).
- <sup>9</sup> A. D. Stoycheva and S. J. Singer, *Phys. Rev. E* **65**, 036706 (2002).
- <sup>10</sup> J. R. Iglesias, S. Goncalves, O. A. Nagel, and M. Kiwi, *Phys. Rev. B* **65**, 064447 (2002).
- <sup>11</sup> The present strategy can be seen to correspond to a ‘phase field’ approach. See L.-Q. Chen, *Annu. Rev. Mater. Sci.* **32**, 113 (2002).
- <sup>12</sup> P. M. Chaikin and T. C. Lubensky, *Principles of Condensed Matter Physics*, (Cambridge University Press, 1995).
- <sup>13</sup> K. L. Babcock and R. M. Westervelt, *Phys. Rev. Lett.* **63**, 175 (1989); K. L. Babcock and R. M. Westervelt, *Phys. Rev. E* **40**, 2022 (1989).
- <sup>14</sup> M. P. de Albuquerque and P. Molho, *J. Magn. Magn. Mat.* **113**, 132 (1992); *ibid.* **140**, 1869 (1995).
- <sup>15</sup> S. Miura, M. Mino, and H. Yamazaki, *J. Phys. Soc. Japan* **70**, 2821 (2001).
- <sup>16</sup> E. A. Jagla, unpublished.
- <sup>17</sup> C. B. Muratov, *Phys. Rev. E* **66**, 066108 (2002).
- <sup>18</sup> J. Swift and P.C. Hohenberg, *Phys. Rev. A* **15**, 319 (1977); M. Bahiana and Y. Oono, *Phys. Rev. A* **41**, 6763 (1990); H. Qian and G. F. Mazenko **67**, 036102 (2003); T. Galla and E. Moro, *Phys. Rev. E* **67**, 035101 (2003).